Operation of High Peak Power Differential Phase Shift Circulators at Direct Magnetic Fields Between Subsidiary and Main Resonances

JOSEPH HELSZAJN, MEMBER, IEEE, AND P. N. WALKER

Abstract—**Instability in high peak power ferrite devices is usually avoided by either widening the spinwave linewidth to move the onset of the subsidiary resonance above the specification of the device, or by using a value of magnetic field below that at which the peak in the subsidiary resonance occurs. A third way to prevent this instability altogether is by adjusting the direct field and material magnetization to prohibit the frequency relation between the microwave signal and the spinwaves. This approach leads to an exceptionally low loss device at both small and large signal levels. The paper describes the experimental development of an 8.5–9.6-GHz 1-MW differential phase shift circulator biased in this way with an insertion loss of less than 0.20 dB.**

I. Introduction

It is well known that ferrite devices exhibit a subsidiary resonance at large signal levels at a direct magnetic field below the main resonance [1]. The subsidiary resonance is power sensitive and leads to a nonlinear insertion loss that limits the peak power rating of ferrite devices. This behavior is well understood [2] and is related to the transfer of power from the microwave magnetic field to spinwaves at half the frequency of the microwave signal. One standard way of avoiding this instability relies on material technology to widen the spinwave linewidth at the expense of the overall small signal insertion loss. A second way to avoid this difficulty is to bias the material below the peak of the subsidiary resonance. Still a third solution to this problem is to ensure that the frequency relation between the microwave signal and the spinwaves at half its frequency cannot be satisfied [2], [3]. This last condition has been employed in [4] in the case of a junction circulator but has not been widely appreciated. The purpose of this paper is to extend this technique in the design of a high power differential phase shift circulator.

The theoretical section of the paper gives a complete definition of the operating characteristics of this type of device in terms of the magnetic variables of the ferrite material. The essential parameters are the direct magnetic field, the separation between the skirts of the subsidiary and main resonances, the bandwidth of this region, and the relation between magnetization and linewidth to ensure that the effective or scalar permeabilities do not take on negative values over the operating band of the device. Since spinwave instability at half the pump frequency is completely suppressed with this design, the uniform mode linewidth may be selected without regard to that of the spinwave one.

The paper includes a detailed study of the region between the subsidiary and main resonances at high peak power for a number of different garnet and ferrite materials, as well as a small signal study of the two senses of phase shift of single waveguide sections. One important advantage of biasing the ferrite material between the subsidiary and main resonances is that the overall magnetic loss is less than it is below the subsidiary resonance, due to the fact that the small signal interaction between the microwave signal and the spinwave manifold is not possible in this region. No consideration has therefore been given in this paper to the effect of spinwave linewidth on the overall insertion loss of the device. The paper describes a prototype 1-MW peak X-band differential phase shift circulator with an insertion loss of 0.18 dB. Although 1-MW differential phase shift circulators have been available commercially at X-band for many years they have been based on advanced material technology which is not the case here, and their designs have usually required a compromise between insertion loss and peak power rating, which again is not the case here. The best commercial insertion loss at 1 MW is of the order of 0.22 dB compared with the value of 0.18 dB obtained with the technique described in this paper.

II. Low Loss Interval Between Subsidiary and Main Resonances

A low loss region has been experimentally observed in ferrite materials at large microwave signal levels between the subsidiary and main resonances [4]. This region is defined in Fig. 1. Its width is of interest and will now be derived. This may be done by forming the difference between the two fields defined by the spinwave dispersion relation and the main resonance.

Manuscript received March 1, 1977; revised October 11, 1977.
J. Helszajn is with the Department of Electrical and Electronic Engineering, Heriot–Watt University, 31-35 Grassmarket, Edinburgh EH1 2HT, Scotland.
P. N. Walker is with Feranti Ltd., Dundee, Scotland.

0018-9480/78/0900-0653$00.75 ©1978 IEEE

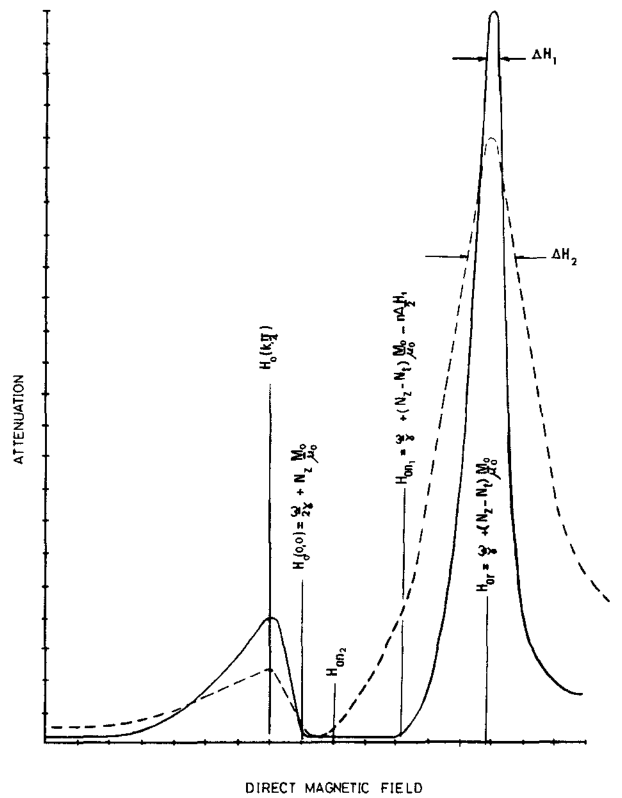

Fig. 1. Subsidiary and main resonances at large signal showing definition of low loss region.

The main resonance is given by Kittel's equation by [7]

$$\omega^2=(\omega_{0r}-N_z\omega_m+N_x\omega_m)(\omega_{0r}-N_z\omega_m+N_y\omega_m) \quad (1)$$

where

$$\omega_{0r}=\gamma H_{0r} \quad (2)$$

$$\omega_m=\gamma M_0/\mu_0. \quad (3)$$

M_0 is the saturation magnetization in $\mathrm{Wb/m^2}$, γ is the gyromagnetic ratio (2.21×10^5 (rad/s)/(A/m)), N_x, N_y, and N_z are the demagnetizing factors, H_{0r} is the direct magnetic field at resonance in A/m, and μ_0 is the free space permeability ($4\pi\times10^{-7}$ H/m).

For an ellipsoidal shaped geometry $N_x=N_y=N_t$ thus (1) becomes

$$\omega=(\omega_{0r}-N_z\omega_m+N_t\omega_m). \quad (4)$$

Rearranging this equation gives

$$H_{0r}=\frac{\omega}{\gamma}+(N_z-N_t)\frac{M_0}{\mu_0}. \quad (5)$$

The field at the edge of the main resonance in Fig. 1 may be written in terms of the uniform mode linewidth as

$$H_{0n}=\frac{\omega}{\gamma}+(N_z-N_t)\frac{M_0}{\mu_0}-\frac{n\Delta H}{2} \quad (6)$$

where the value of n is determined by the line shape.

For the subsidiary resonance the frequency relation $\omega_k=\omega/2$ is satisfied provided [2]

TABLE I

MATERIAL	M_0 wb/m²	ΔH A/m	ΔH_k A/m	ε′	T_c
• (1) G500	·0550	5172	285	14·4	180
• (2) G1021	0·1100	7162	435	15·2	280
• (3) G1210	0·1200	3183	110	14·8	220
* (4) C 20	0·1850	34218	—	11·4	520

* MANUFACTURED BY COUNTIS
• MANUFACTURED BY TRANS-TECH

$$\gamma H_{ex}a^2k^2=\tfrac{1}{2}(\omega_m^2\sin^4\theta_k+\omega^2)^{1/2}-\tfrac{1}{2}\omega_m\sin^2\theta_k-\gamma H_0+N_z\omega_m \quad (7)$$

where k is the spinwave number, θ_k is the angle between the spinwaves and the direct field H_0, H_{ex} is the exchange field, and a is the lattice constant.

The dispersion relation ceases to yield a real value for k with $\theta_k=0$ at a field given by

$$H_0(k,\theta_k)=H_0(0,0)=\frac{\omega}{2\gamma}+N_z\frac{M_0}{\mu_0}. \quad (8)$$

The field $H_0(0,0)$ determines the upper skirt of the subsidiary resonance region.

The width of the low loss window is obtained by taking the difference between (6) and (8):

$$\delta H=\frac{\omega}{2\gamma}-N_t\frac{M_0}{\mu_0}-n\frac{\Delta H}{2}. \quad (9)$$

This relation must be satisfied subject to (14) which gives the relation between the magnetization and the uniform mode linewidth. Equation (9) is that given in reference [4] except for the linewidth term.

Good agreement between the theory and experiment is obtained by taking $n=12$ in (9) for the ferrite material and $n=20$ for the garnet materials in Table I. The direct field H_0 at ω_0 is selected such that it lies in the middle of the low loss region.

$$H_0=\frac{H_0(0,0)+H_{0n}}{2}. \quad (10)$$

In terms of the original variables.

$$H_0=\frac{3\omega_0}{4\gamma}+\left(N_z-\frac{N_t}{2}\right)\frac{M_0}{\mu_0}-\frac{n\Delta H}{4} \quad (11)$$

where ω_0 is the center frequency in rad/s. Using the magnetization given by (14) in (11) with $n=20$, $N_z=0.80$, $N_t=0.10$ gives H_0 as 2.37×10^5 A/m at 9.6 GHz.

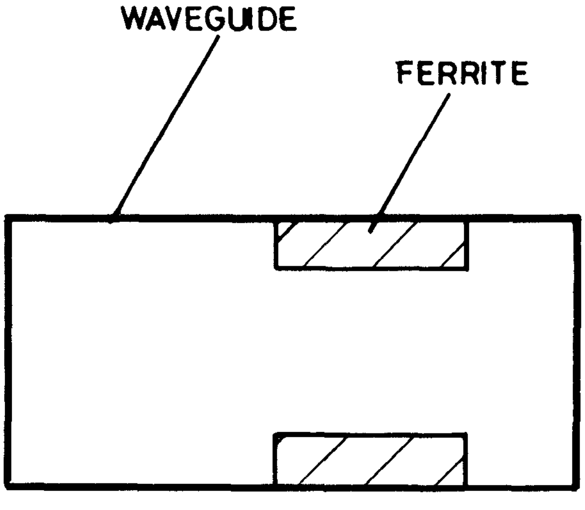

Fig. 2. Schematic diagram of waveguide differential phase shift geometry.

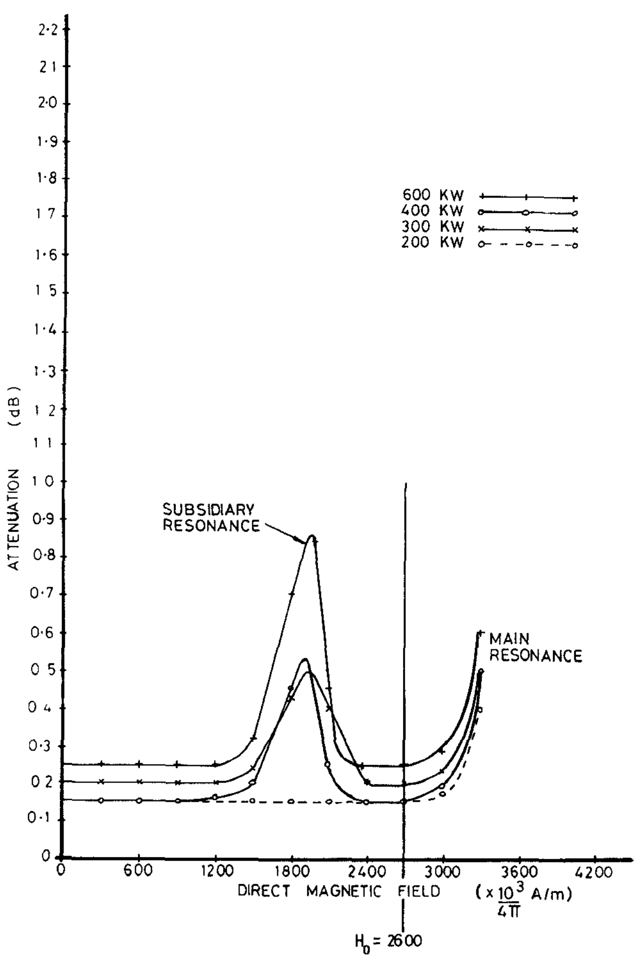

Fig. 3. Subsidiary and main resonances for 8.25×1.52×152-mm garnet with M_0=0.0550 Wb/m^2 and ΔH=5172 A/m.

III. Magnetization

Since the applied direct field defined by (10) exceeds that required to saturate the material it is necessary to ensure that the ferrite parameters do not lead to negative values of effective or circular permeabilities over the

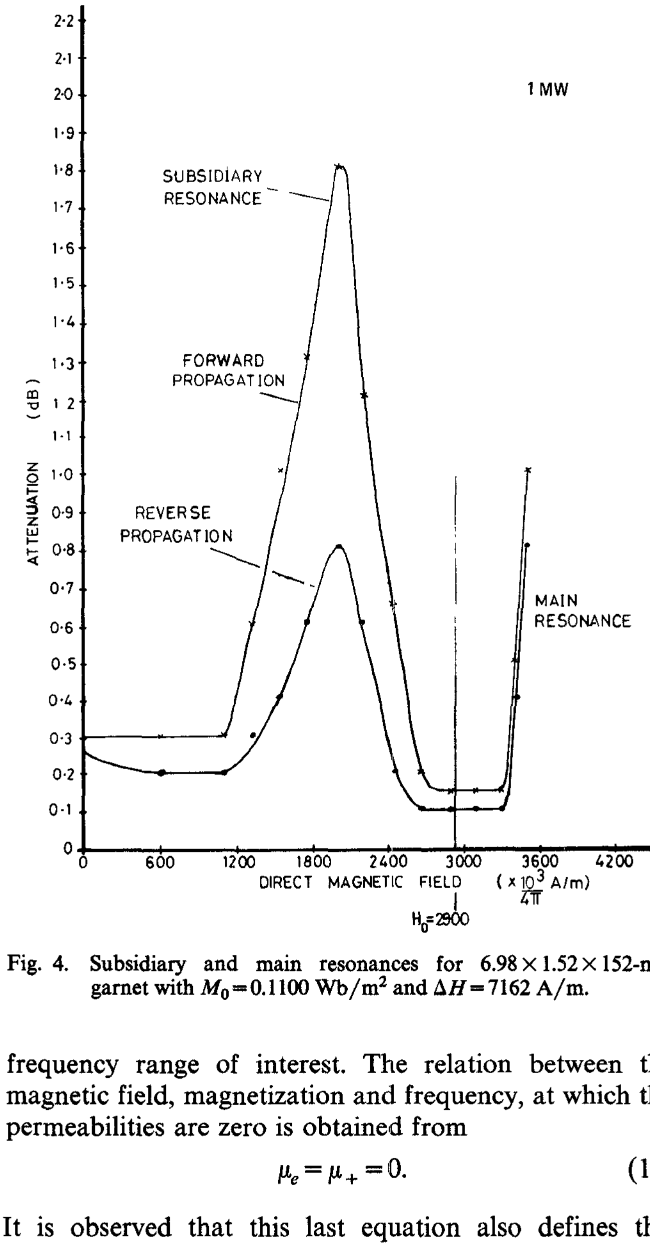

Fig. 4. Subsidiary and main resonances for 6.98×1.52×152-mm garnet with M_0=0.1100 Wb/m^2 and ΔH=7162 A/m.

frequency range of interest. The relation between the magnetic field, magnetization and frequency, at which the permeabilities are zero is obtained from

$$\mu_e = \mu_+ = 0. \tag{12}$$

It is observed that this last equation also defines the condition $K/\mu = 1$. In the terms of the original variables the preceding equation gives

$$\frac{\gamma M_0}{\mu_0} + \gamma H_0 - N_z \frac{\gamma M_0}{\mu_0} - \omega = 0. \tag{13}$$

This equation must be evaluated at ω_1 with H_0 defined at ω_0 by (10).

$$\frac{\gamma M_0}{\mu_0}\left(1 - \frac{N_t}{2}\right) = \omega_1 - \frac{3\omega_0}{4} + \frac{n\gamma\Delta H}{4}. \tag{14}$$

The preceding equation defines the maximum magnetization of the ferrite material in terms of the center and lower bandedge frequencies of the specification of the device.

Applying the above equation to the design of a circulator with a center frequency of 9.6 GHz and a lower bandedge of 9.0 GHz gives M_0 as 0.1150 Wb/m^2 for $n=20$, $\Delta H=7160$ A/m, and $N_t \approx 0.10$.

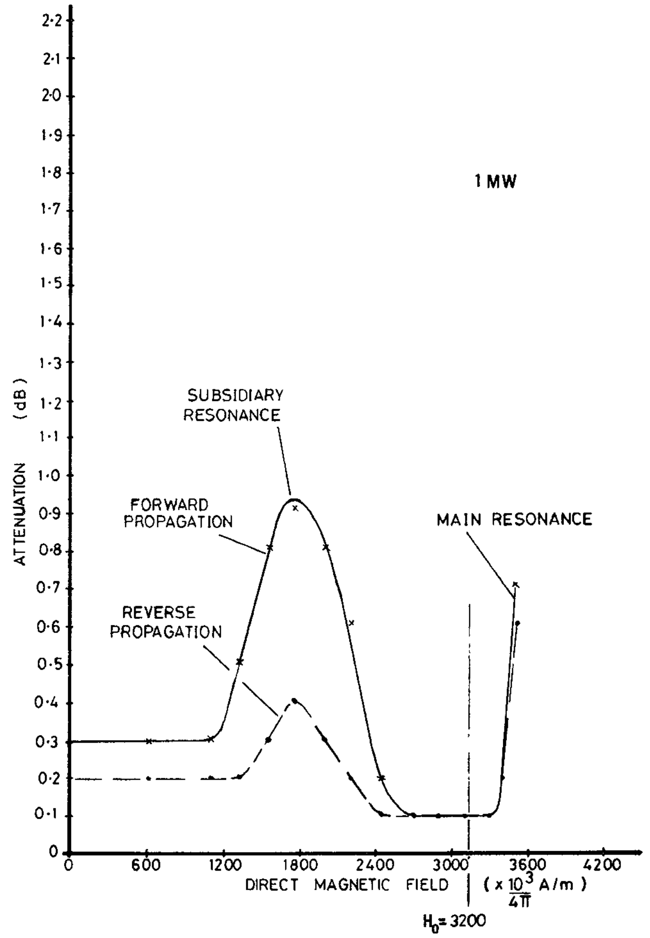

Fig. 5. Subsidiary and main resonances for 6.98×1.52×152-mm garnet with $M_0=0.1200$ Wb/m^2 and $\Delta H=3183$ A/m.

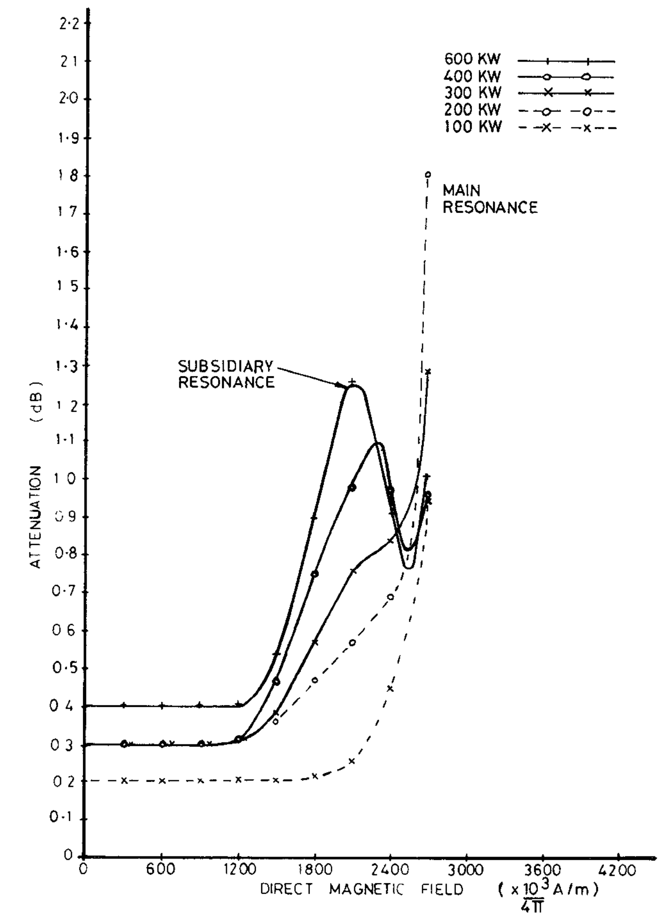

Fig. 6. Subsidiary and main resonances for 8.25×1.52×152-mm ferrite with $M_0=0.1850$ Wb/m^2 and $\Delta H=34{,}218$ A/m.

IV. Bandwidth

One important parameter in any device is its bandwidth. This parameter may be obtained by fixing the direct magnetic field at the value given by (11) and replacing ω by $\omega_{1,2}$ in (6) and (8). Thus

$$H_0=\frac{\omega_1}{\gamma}+(N_z-N_t)\frac{M_0}{\mu_0}-\frac{n\Delta H}{2} \quad (15)$$

$$H_0=\frac{\omega_2}{2\gamma}+N_z\frac{M_0}{\mu_0}. \quad (16)$$

Rearranging the preceding equations gives the bandwidth as

$$\omega_2-\omega_1=\frac{2\gamma}{3}\left(\frac{\omega_0}{\gamma}-2N_t\frac{M_0}{\mu_0}-n\Delta H\right). \quad (17)$$

Introducing the material parameters defined by (11) and (14) in (17) with $n=20$, $N_z=0.80$, $N_t=0.10$ gives f_2-f_1 as 2.6 GHz at 9.6 GHz. This value of bandwidth being compatible with most X-band requirements.

V. Experimental Data on Low Loss Region

This section summarizes experimental data at large peak power obtained on a differential phase shift section in a single 152-mm long waveguide using a number of different ferrite and garnet materials (see Fig. 2). The materials selected have a range of saturation magnetization from 0.0550–0.1850 Wb/m^2, a range of linewidth from 3.2×10^3–3.4×10^4 A/m, and a spinwave linewidth between 110–285 A/m. The peak power was varied in 100-kW steps up to 600 kW at a fixed frequency of 9.3 GHz and in the case of materials 2 and 3, the peak power was increased to 1 MW at a frequency of 9.6 GHz. The direct magnetic field was varied from zero to the skirt of the main resonance. The results obtained in this manner are illustrated in Figs. 3–6 inclusive.

Figs. 3–6 clearly illustrate a low loss region at high peak power between the subsidiary and main resonances. Fig. 6 indicates the importance of the uniform linewidth in defining the region between the subsidiary and main resonances. Figs. 4 and 5 illustrate how, by the correct choice of material, a low loss region is defined with an insertion loss less than that below the subsidiary resonance. One explanation for this characteristic lower loss between the subsidiary and main resonances is the absence of coupling between the microwave signal at both small and large signal levels to spinwaves at half the pump frequency. While no such observation has appeared in the literature, it is well known that the uniform mode linewidth passes thru a maximum when the uniform mode is degenerate with spinwaves at the same frequency [5], [6].

Fig. 3 represents an earlier result which although it does not display the latter property nevertheless is not believed

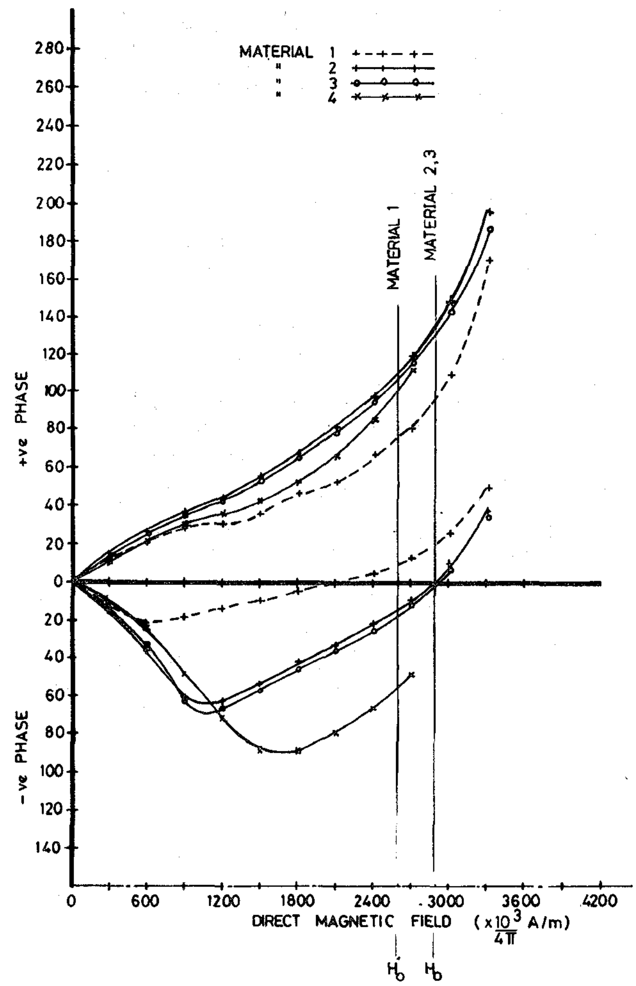

Fig. 7. Differential phase shift for different materials for 8.25×1.52×152-mm garnets.

to invalidate what is assumed to be a general characteristic. It is reproduced here because it serves to illustrate the influence of the uniform linewidth and saturation magnetization on the region between the subsidiary and main resonances.

It is observed that material 2 in Table I most nearly conforms to the calculation in the theoretical sections.

VI. Differential Phase Shift Sections

Differential phase shift circulators rely for their operation on a nonreciprocal differential phase shift of 90 degrees between the magic tee and 3-dB hybrid of the device. To take advantage of the low loss region between the subsidiary and main resonances in the design of the phase shift section the direct magnetic field necessary to obtain the required differential phase shift must be compatible with (11).

Fig. 7 depicts the differential phase shift versus the direct magnetic field for 3 garnets and 1 ferrite materials of similar cross sections.

It is observed that by operating above subsidiary resonance, the differential phase shift is now changing very little with magnetic field. This can be seen clearly in Fig. 7 where in every case the $-ve$ phase reaches saturation magnetization and then runs almost parallel to the $+ve$ phase. This means that the device is less sensitive to change in direct field than it is below subsidiary resonance device.

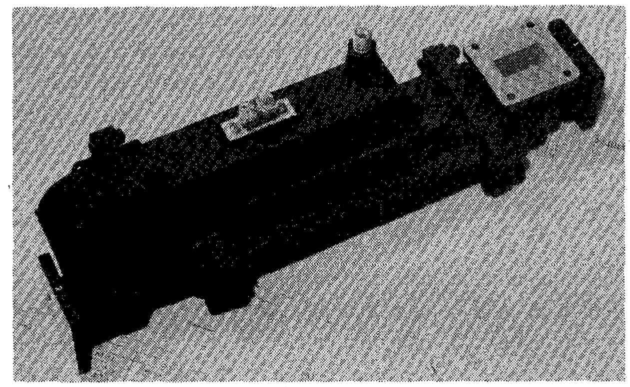

Fig. 8. 1-MW differential phase shift circulator using 6.98×1.52×144-mm garnet.

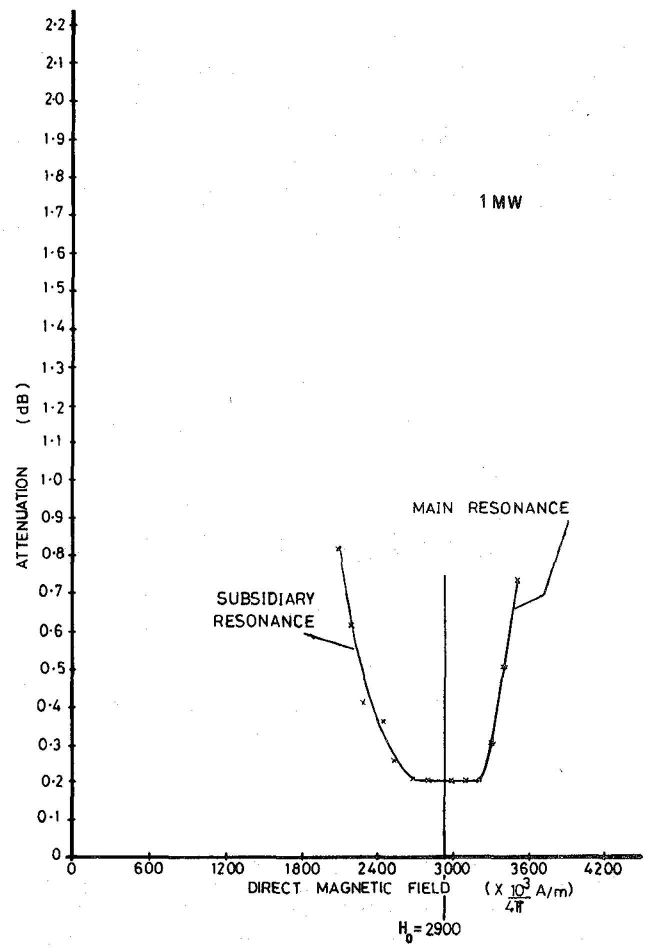

Fig. 9. Insertion loss of assembled differential phase shift circulator at 1-MW signal level for garnet 2.

VII. 1-MW Differential Phase-Shift Circulator

Fig. 8 illustrates a waveguide differential phase-shift circulator using phase-shift sections working at a direct magnetic field between the subsidiary and main resonances. Samarium cobalt magnets are used for compactness. The input and output waveguides of the circulator and the phase-shift sections are all in WR112 waveguide.

Its overall length is 320 mm. The small signal isolations of this circulator are better than 20 dB between all isolated ports over 8.5–9.6 GHz with a small signal insertion loss below 0.20 dB over the temperature range $-40-+100°C$. Fig. 9 indicates the large signal insertion loss of the differential phase shift circulator at a peak power level of 1 MW at a frequency of 9.6 GHz. The pulsewidth of the signal was 0.16 μs and its duty cycle was 0.001.

It is seen from the above results that not only is the insertion loss of the device independent of signal level up to 1-MW peak but also that this biasing condition minimizes the magnetic losses of the material due to the suppression of both small and large signal coupling between the microwave signal and the spinwave manifold.

VIII. Conclusions

This paper has described the successful design of a 1-MW differential phase shift circulator using ferrite sections biased at a direct magnetic field between the subsidiary and main resonances. Although the final device has been evaluated at 1 MW (500 kW through each phase shift section), the individual phase shift sections exhibited no nonlinear loss at 1-MW peak. This proves the design of such a circulator to a power rating of 2-MW peak. The overall insertion loss of the final device was 0.18 dB at 9.6 GHz.

Acknowledgment

The authors would like to thank Ferranti Ltd., Dundee, for permission to publish this paper.

References

[1] R. W. Damon, "Relaxation effects in ferromagnetic resonance," *Rev. Mod. Phys.*, vol. 25, pp. 239–45, 1953.
[2] H. Suhl, "The non-linear behaviour of ferrites at high signal level," *Proc. Inst. Radio Engrs.*, vol. 44, p. 1270, 1956.
[3] E. Schlömann, "Ferromagnetic resonance at high power levels," Raytheon Technical Report R-48, 1959.
[4] A. Lagrange, H. Lahmi, and B. R. Vallatin, "*K*-band high-peak-power junction circulator: Influence of the static magnetic field," *IEEE Trans. Magnetics*, vol. Mag-9, pp. 531–534, Sept. 1973.
[5] C. R. Buffler, *J. Appl. Phys.*, vol. 30, p. 1725, 1959.
[6] Q. H. F. Vrehen, G. H. Beljers, and J. G. M. de Lau, "Microwave Properties Fine-Grain Ni and Mg Ferrites," *IEEE Trans. Magnetics*, MAG-5, pp. 617–621, 1969.
[7] C. Kittel, "On the theory of ferromagnetic resonance absorption," *Phys. Rev.*, vol. 73, pp. 155–161, 1948.

Design Considerations of Broadband Dual-Mode Optical Fibers

JUN-ICHI SAKAI, KENICHI KITAYAMA, MEMBER, IEEE, MASAHIRO IKEDA, MEMBER, IEEE, YASUYUKI KATO, AND TATSUYA KIMURA, MEMBER, IEEE

***Abstract*—We propose and present design data for a new type of graded index fiber which has a profile and radius such that only two mode groups (LP_{01} and LP_{11}) propagate and both propagate with virtually identical group velocities. This dual-mode fiber has a core diameter approximately twice that of a conventional step-index single-mode fiber. For example, a core diameter of 16.3 μm is attainable with relative index difference $\Delta=0.3$ percent at 1.25-μm wavelength. Fabrication tolerances securing a group delay difference below 100 ps/km are given by a power-law profile parameter $\alpha=4.85\pm0.25$ and a normalized frequency $v=4.45\pm0.11$. The allowable v-value deviation range to keep the group delay difference within 100 ps/km is about five times as large as that of a step-index fiber, in which group delays of two mode groups are matched. Comparison with a multimode graded-index fiber, with respect to group delay characteristics and bending loss of the dual-mode fiber, are also discussed.**

Manuscript received November 10, 1977; revised February 6, 1978.
J. I. Sakai and T. Kimura are with the Musashino Electrical Communication Laboratory, Nippon Telegraph and Telephone Public Corporation, Musashino-shi, Tokyo, 180, Japan.
K. Kitayama, M. Ikeda, and Y. Kato are with the Ibaraki Electrical Communication Laboratory, Nippon Telegraph and Telephone Public Corporation, Tokai, Ibaraki, 319-11, Japan.

I. Introduction

SINGLE-MODE optical fibers are expected to offer a promising means for large-capacity optical transmission. However, technical difficulties in fiber splicing and coupling seem to have blocked their utilization, because the core diameter is as small as several microns. Several methods to enlarge the core diameter have been devised.

One method is to decrease the relative index difference Δ between core and cladding. It has been reported that Δ has been lowered to the order of 0.1 percent [1]. However, the bending losses increase with decreasing Δ. Another recognized method is to use an optical carrier with longer wavelengths [2] than the currently used 0.8–0.9 μm. When the carrier wavelength is chosen between 1.0 and 1.6 μm,

0018-9480/78/0900-0658$00.75 ©1978 IEEE